Bottomonium suppression in heavy-ion collisions

Michael Strickland
Kent State University
Kent, OH USA

N. Brambilla, M.-A. Escobedo, M.S., A. Vairo,
P. Vander Griend, and J.H. Weber, arXiv:2012.01240 and forthcoming

Quarkonia meet Dark Matter
June 18, 2021

Bottomonium Suppression

- In a high temperature quark-gluon plasma we expect **weaker color binding** (Debye screening + asymptotic freedom)

E. V. Shuryak, Phys. Rept. 61, 71–158 (1980)
T. Matsui, and H. Satz, Phys. Lett. B178, 416 (1986)
F. Karsch, M. T. Mehr, and H. Satz, Z. Phys. C37, 617 (1988)

- Also, high energy plasma particles which slam into the bound states cause them to have shorter lifetimes → **larger spectral widths**

TUMQCD Collaboration, 1804.10600

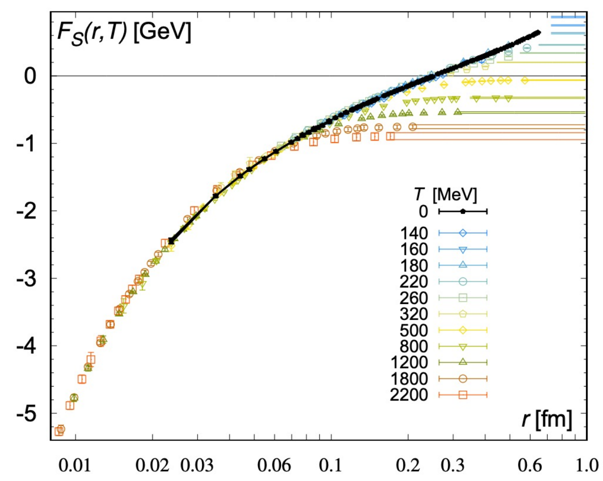

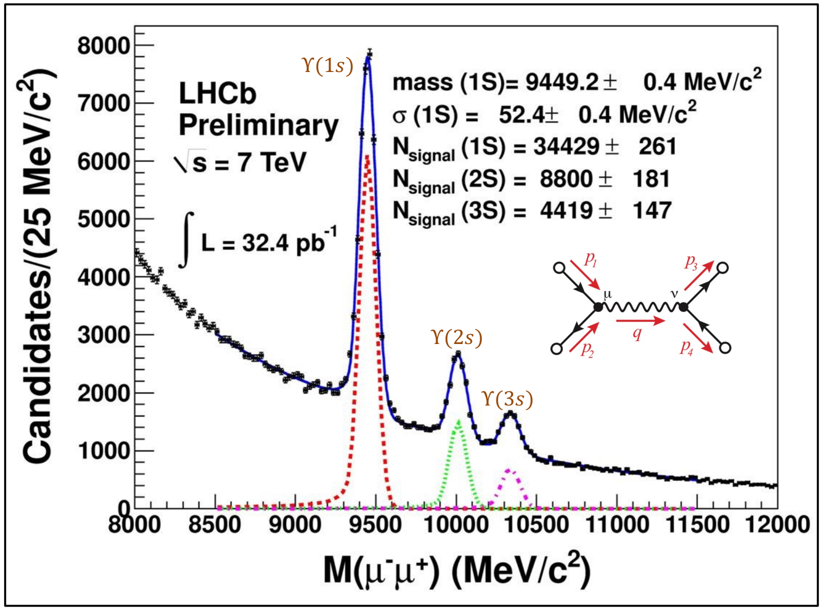

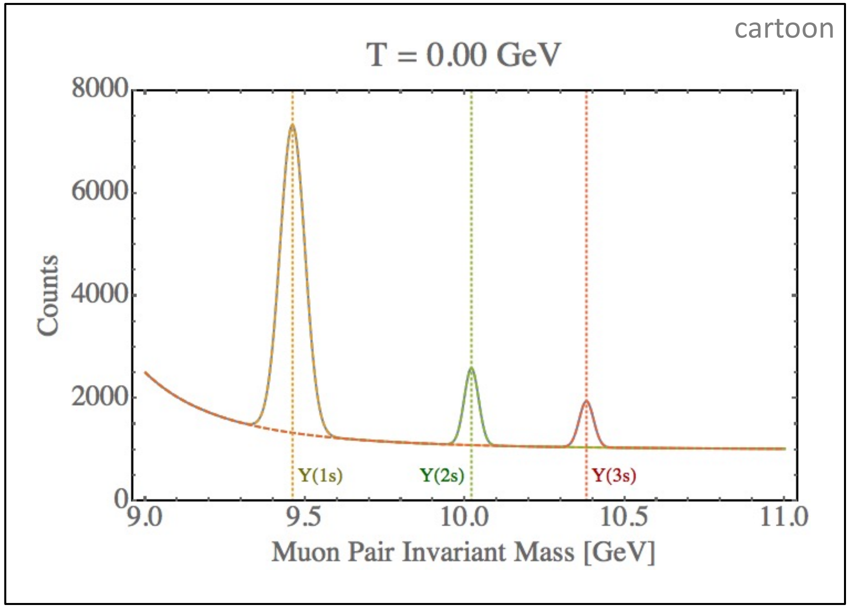

Bottomonium Suppression

- In a high temperature quark-gluon plasma we expect **weaker color binding** (Debye screening + asymptotic freedom)

E. V. Shuryak, Phys. Rept. 61, 71–158 (1980)
T. Matsui, and H. Satz, Phys. Lett. B178, 416 (1986)
F. Karsch, M. T. Mehr, and H. Satz, Z. Phys. C37, 617 (1988)

- Also, high energy plasma particles which slam into the bound states cause them to have shorter lifetimes → **larger spectral widths**

TUMQCD Collaboration, 1804.10600

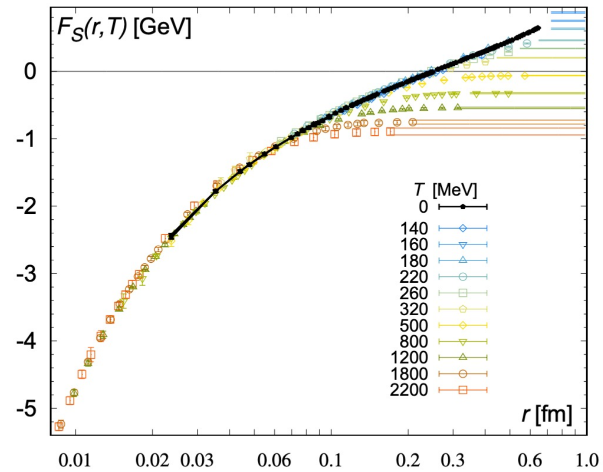

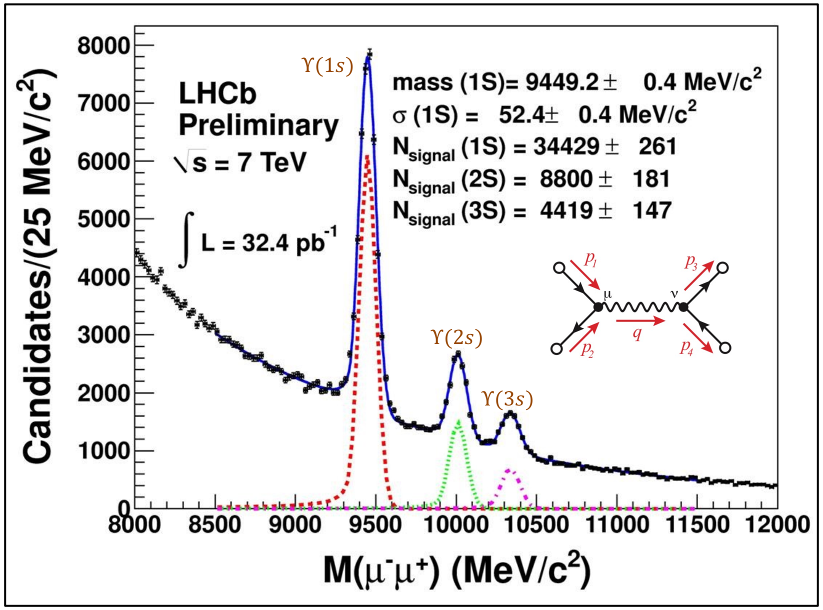

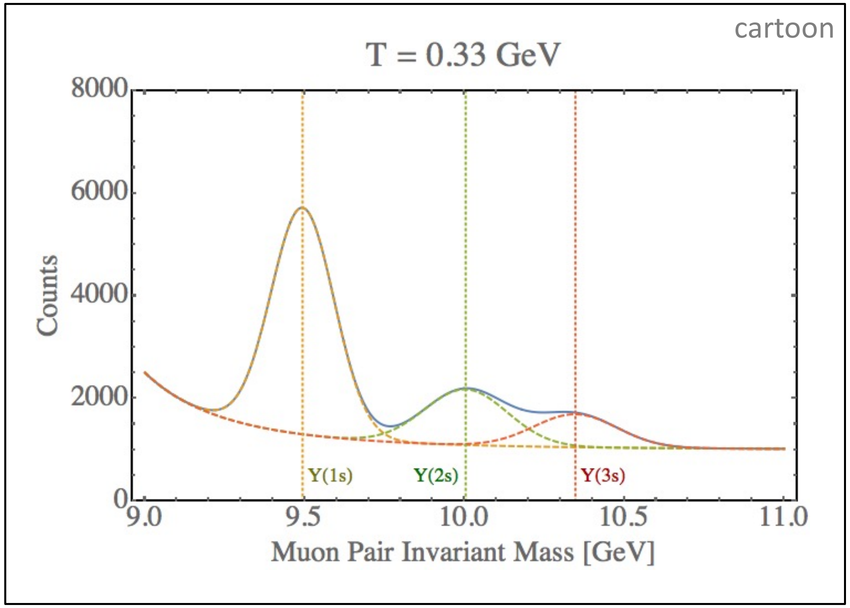

Bottomonium Suppression

- In a high temperature quark-gluon plasma we expect **weaker color binding** (<u>Debye screening</u> + asymptotic freedom)

E. V. Shuryak, Phys. Rept. 61, 71–158 (1980)
T. Matsui, and H. Satz, Phys. Lett. B178, 416 (1986)
F. Karsch, M. T. Mehr, and H. Satz, Z. Phys. C37, 617 (1988)

- Also, high energy plasma particles which slam into the bound states cause them to have shorter lifetimes → **larger spectral widths**

TUMQCD Collaboration, 1804.10600

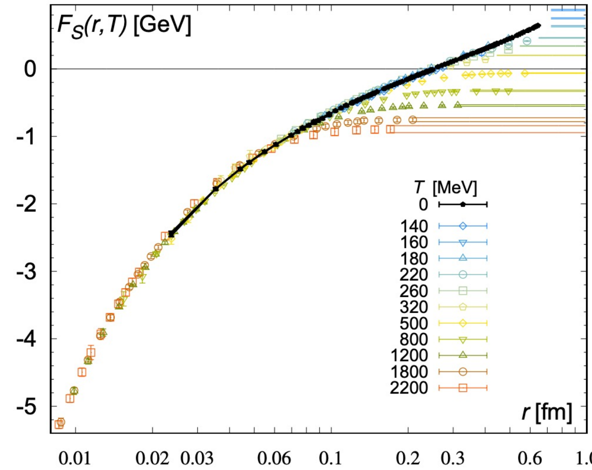

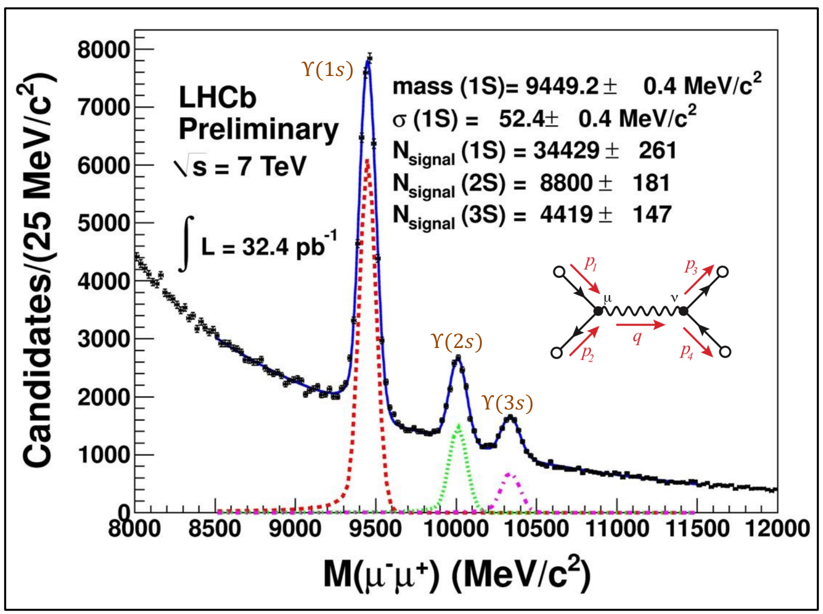

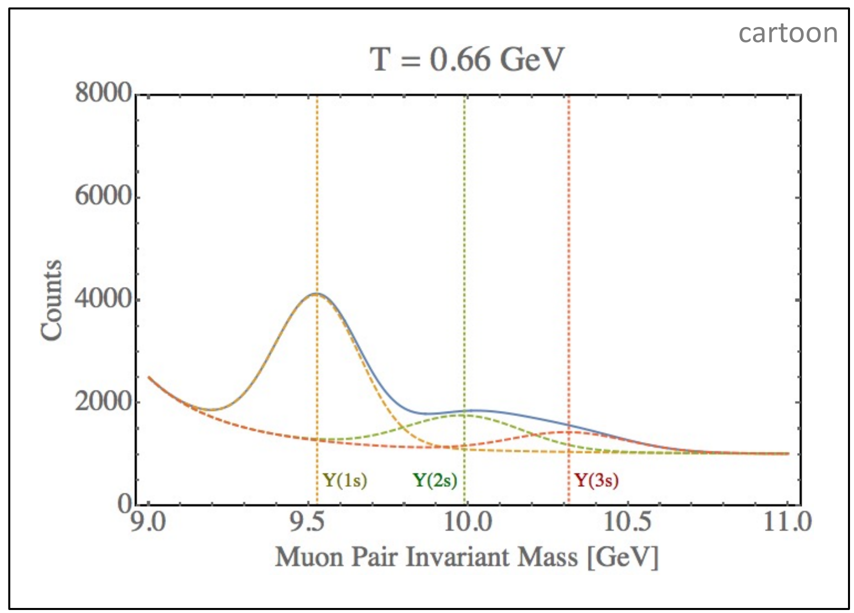

Bottomonium Suppression

- In a high temperature quark-gluon plasma we expect **weaker color binding** (Debye screening + asymptotic freedom)

E. V. Shuryak, Phys. Rept. 61, 71–158 (1980)
T. Matsui, and H. Satz, Phys. Lett. B178, 416 (1986)
F. Karsch, M. T. Mehr, and H. Satz, Z. Phys. C37, 617 (1988)

- Also, high energy plasma particles which slam into the bound states cause them to have shorter lifetimes → **larger spectral widths**

TUMQCD Collaboration, 1804.10600

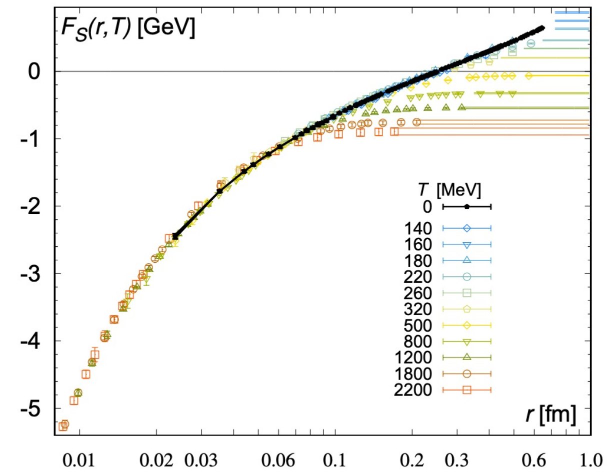

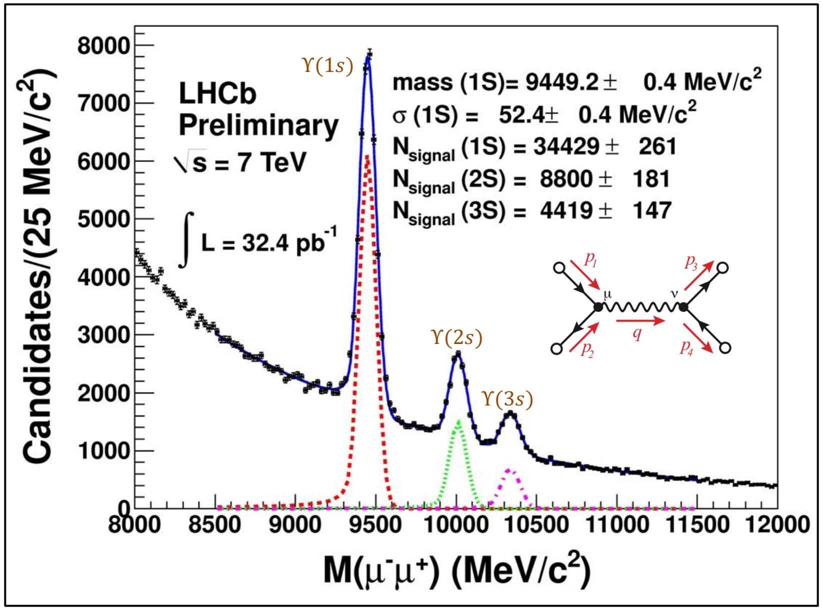

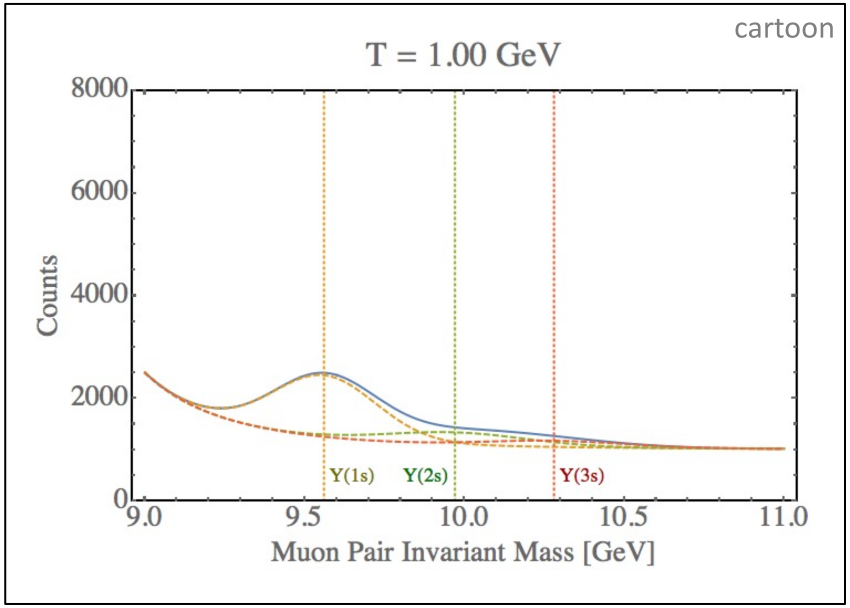

Experimental data – 5.02 TeV Dimuon Spectra

The **CMS, ALICE,** and **ATLAS** experiments have measured bottomonium production in both pp and Pb-Pb collisions. Here I show CMS results.

pp

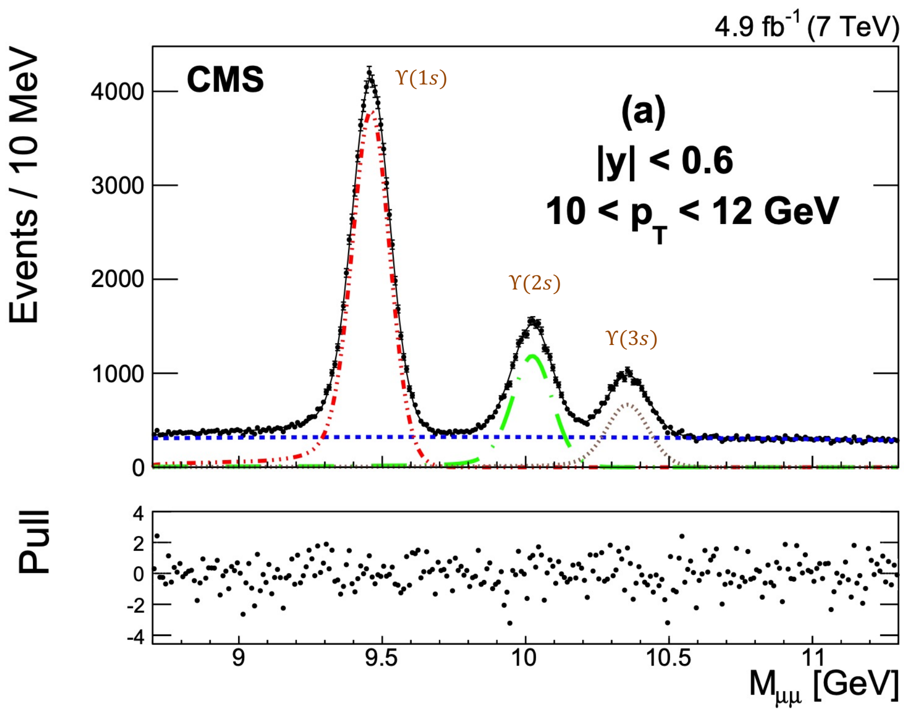

PbPb

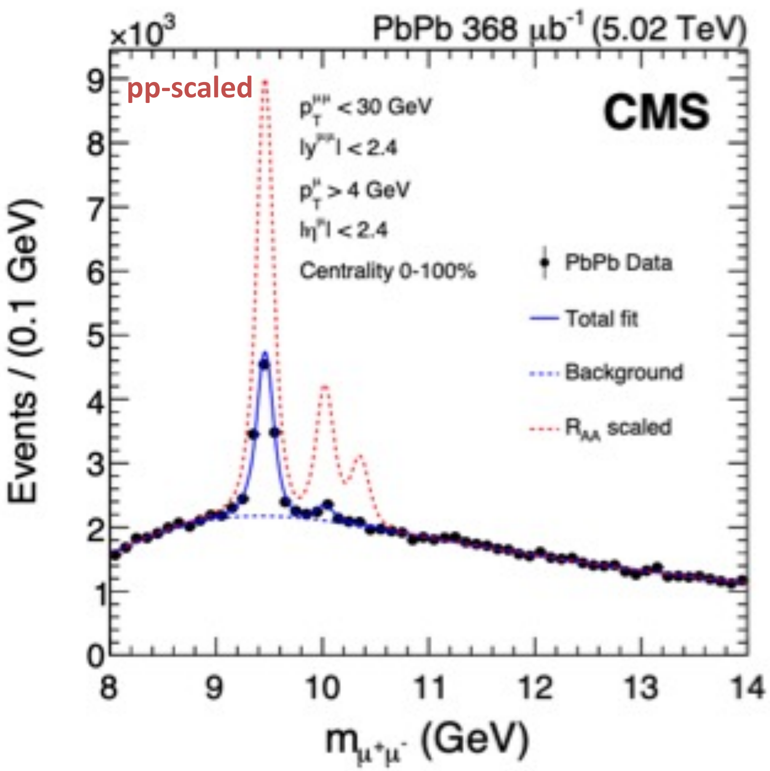

Experimental data – 5.02 TeV Dimuon Spectra

The **CMS, ALICE,** and **ATLAS** experiments have measured bottomonium production in both pp and Pb-Pb collisions. Here I show CMS results.

pPb

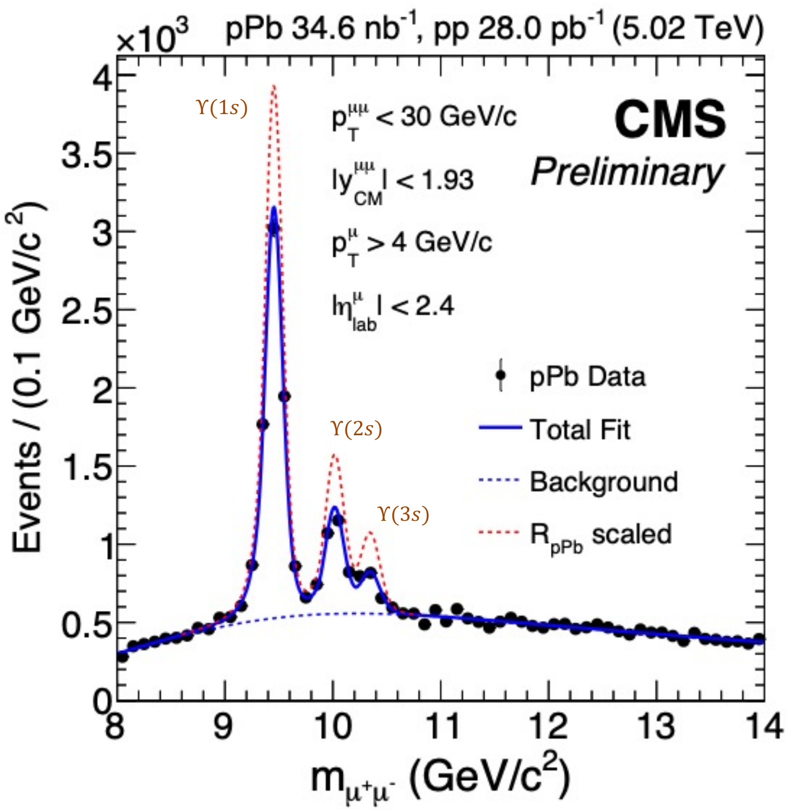

PbPb

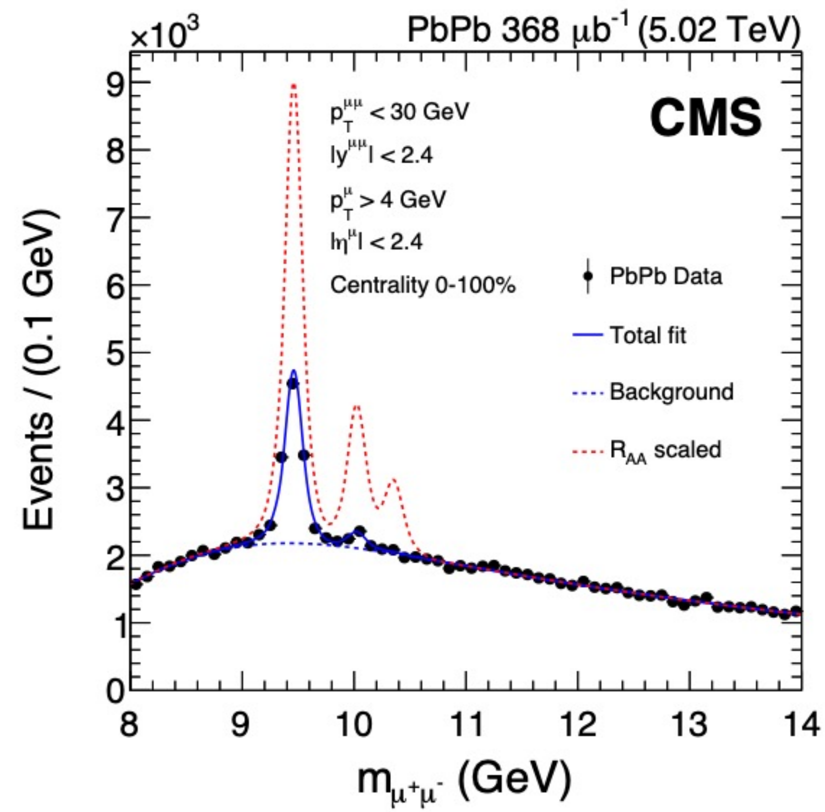

Bottomonia are excellent probes of the QGP

- Can trust heavy quark effective theory more.
- Cold nuclear matter (CNM) effects in AA decrease with increasing quark mass.
- The masses of bottomonia (m ~ 10 GeV) are much higher than the temperature generated in HICs (T < 1 GeV) → bottomonium production dominated by initial hard scatterings.
- Both closed and open bottom production is quite rare in RHIC and LHC energy HICs → the probability for regeneration of bottomonia through statistical recombination is much smaller than for charm quarks; less model uncertainty.
[see e.g. E. Emerick, X. Zhao, and R. Rapp, arXiv:1111.6537 and others]

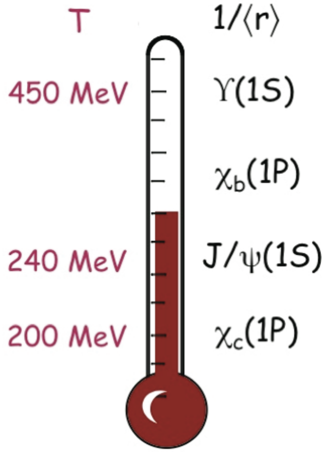

A. Mocsy, P. Petreczky, and MS, 1302.2180

Conceptual problem

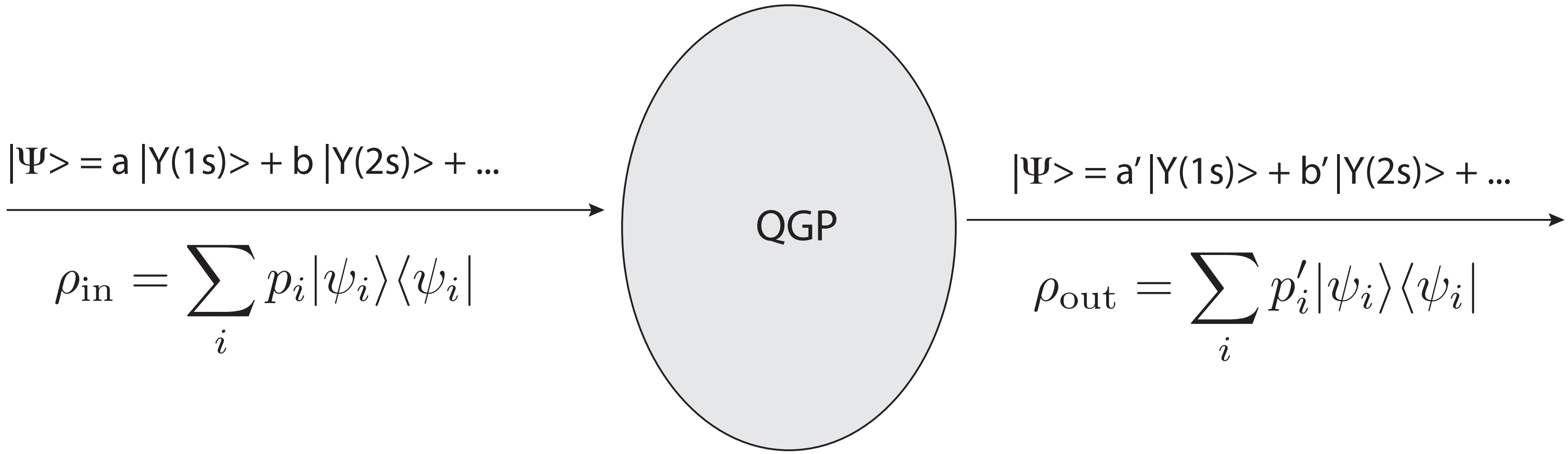

- Bottomonium states have a large binding energy and are produced locally (hard processes) at early times in hard collisions (t < 1 fm/c).
- They then propagate through the plasma and interact with the medium.
- Bound states can break up and potentially re-form due to in-medium transitions induced by in-medium gluon absorption and emission.

Conceptual problem

|Ψ> = a |Y(1s)> + b |Y(2s)> + ...

$$\rho_{\rm in} = \sum_i p_i |\psi_i\rangle\langle\psi_i|$$

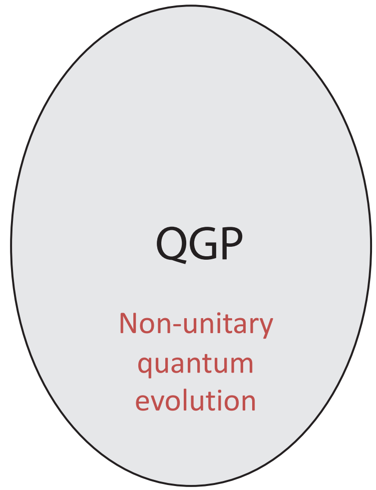

|Ψ> = a' |Y(1s)> + b' |Y(2s)> + ...

$$\rho_{\rm out} = \sum_i p'_i |\psi_i\rangle\langle\psi_i|$$

- Bottomonium states have a large binding energy and are produced locally (hard processes) at early times in hard collisions (t < 1 fm/c).
- They then propagate through the plasma and interact with the medium.
- Bound states can break up and potentially re-form due to in-medium transitions induced by in-medium gluon absorption and emission.

Open quantum system (OQS) approach

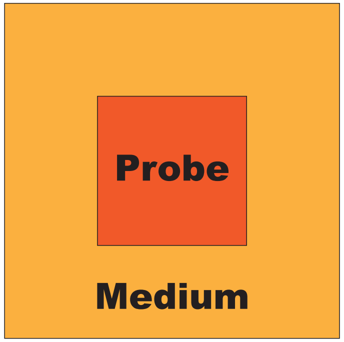

See talks in this workshop by A. Vairo and M. Escobedo

Probe = heavy-quarkonium state

Medium = light quarks and gluons that comprise the QGP

- Can treat heavy quarkonium states propagating through QGP using an open quantum system approach

$$H_{\rm tot} = H_{\rm probe} \otimes I_{\rm medium} + I_{\rm probe} \otimes H_{\rm medium} + H_{\rm int}$$

- Total density matrix

$$\rho_{\rm tot} = \sum_k \frac{1}{Z_{\rm tot}} e^{-E_k/T} |E_k\rangle\langle E_k| \longrightarrow \frac{d}{dt}\rho_{\rm tot} = -i[H_{\rm tot}, \rho_{\rm tot}]$$

- Reduced density matrix

$$\rho_{\rm probe} = {\rm Tr}_{\rm medium}[\rho_{\rm tot}] \longrightarrow$$ **Evolution equation?**

The Lindblad equation

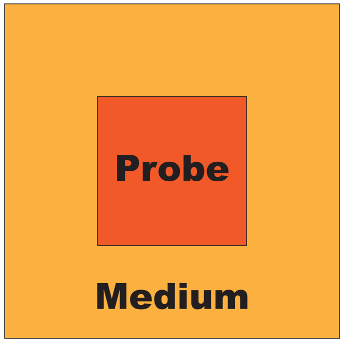

Probe = heavy-quarkonium state

Medium = light quarks and gluons that comprise the QGP

- Separation of time scales
  - Medium relaxation time scale $\langle \hat{O}_{\rm M}(t)\hat{O}_{\rm M}(0)\rangle \sim e^{-t/t_{\rm M}}$
  - Intrinsic probe time scale $t_P \sim \dfrac{1}{\omega_i - \omega_j}$
  - Probe relaxation time scale $\langle p(t)\rangle \sim e^{-t/t_{\rm rel}}$

Lindblad equation

$$t_{\rm rel}\,,\, t_{\rm P} \gg t_{\rm M} \longrightarrow \boxed{\frac{d\rho_{\rm probe}}{dt} = -i[H_{\rm probe}, \rho_{\rm probe}] + \sum_n \left(C_n\, \rho_{\rm probe}\, C_n^\dagger - \frac{1}{2}\{C_n^\dagger C_n, \rho_{\rm probe}\}\right)}$$

- Trace preserving
- Completely positive
- In general, non-unitary evolution

G. Lindblad, Commun. Math. Phys. 48 (1976) 119
V. Gorini, et.al. J. Math. Phys. 17 (1976) 821

OQS + pNRQCD → Lindblad equation

- What are the relevant scales?
  - Temperature T
  - Bound state mass $m \gg T$
  - Bound state size $r \sim mv \sim a_0$ (Bohr radius)
  - Debye mass m_D
  - Binding energy $E \sim mv^2$

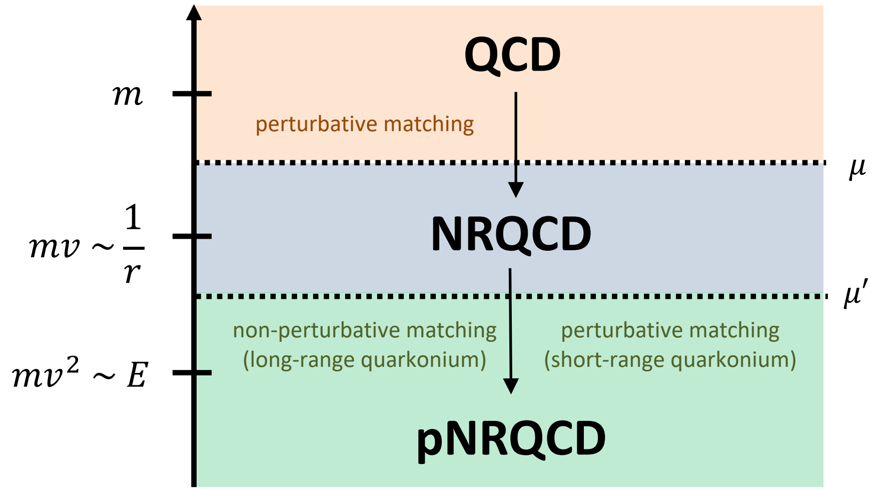

- Separation of time scales
  - Medium relaxation time scale $\langle \hat{O}_{\rm M}(t)\hat{O}_{\rm M}(0)\rangle \sim e^{-t/t_{\rm M}} \to \frac{1}{T}$
  - Intrinsic probe time scale $t_P \sim \dfrac{1}{\omega_i - \omega_j} \to \dfrac{1}{E}$
  - Probe relaxation time scale $\langle p(t)\rangle \sim e^{-t/t_{\rm rel}} \to \dfrac{1}{\text{self-energy}} \sim \dfrac{1}{\alpha_s a_0^2 \Lambda^3}$ $\quad \Lambda = T, E$

$$1/r \gg T \sim m_D \gg E \quad \xrightarrow[t_{\rm rel}\,,\, t_{\rm P} \gg t_{\rm M}]{} \quad \boxed{\frac{d\rho_{\rm probe}}{dt} = -i[H_{\rm probe}, \rho_{\rm probe}] + \sum_n \left(C_n\, \rho_{\rm probe}\, C_n^\dagger - \frac{1}{2}\{C_n^\dagger C_n, \rho_{\rm probe}\} \right)}$$

Lindblad equation

N. Brambilla, M. A. Escobedo, J. Soto and A. Vairo, 1612.07248, 1711.04515

OQS + pNRQCD – Lindblad reorganization

$$\boxed{\frac{d\rho_{\rm probe}}{dt} = -i[H_{\rm probe}, \rho_{\rm probe}] + \sum_n \left(C_n\, \rho_{\rm probe}\, C_n^\dagger - \frac{1}{2}\{C_n^\dagger C_n, \rho_{\rm probe}\} \right)}$$

- $H_{\rm probe}$ is a Hermitian operator (includes singlet and octet states)
- C_n are the **collapse (or jump) operators** (connect different internal states)
- Partial and **total decay widths** are

$$\Gamma_n = C_n^\dagger C_n \qquad \Gamma = \textstyle\sum_n \Gamma_n$$

- Can reorganize Lindblad equation by defining

$$\boxed{H_{\rm eff} = H_{\rm probe} - \frac{i}{2}\Gamma}$$ ← **Non-Hermitian effective Hamiltonian**

$$\longrightarrow \quad \boxed{\frac{d\rho_{\rm probe}}{dt} = -iH_{\rm eff}\rho_{\rm probe} + i\rho_{\rm probe}H_{\rm eff}^\dagger + \sum_n C_n\, \rho_{\rm probe}\, C_n^\dagger}$$

OQS+pNRQCD Hamiltonian and collapse operators

N. Brambilla, M. A. Escobedo, J. Soto and A. Vairo, 1612.07248, 1711.04515

$$\frac{d\rho_{\rm probe}}{dt} = -iH_{\rm eff}\rho_{\rm probe} + i\rho_{\rm probe}H_{\rm eff}^\dagger + \sum_n C_n\,\rho_{\rm probe}\,C_n^\dagger$$

$$\rho = \begin{pmatrix} \rho_s & 0 \\ 0 & \rho_o \end{pmatrix}$$

$$H_{\rm probe} = \begin{pmatrix} h_s & 0 \\ 0 & h_o \end{pmatrix} + \frac{r^2}{2}\gamma \begin{pmatrix} 1 & 0 \\ 0 & \frac{N_c^2-2}{2(N_c^2-1)} \end{pmatrix}$$

mass shift

$$C_i^0 = \sqrt{\frac{\kappa}{N_c^2-1}}\, r^i \begin{pmatrix} 0 & 1 \\ \sqrt{N_c^2-1} & 0 \end{pmatrix},$$

$$C_i^1 = \sqrt{\frac{(N_c^2-4)\kappa}{2(N_c^2-1)}}\, r^i \begin{pmatrix} 0 & 0 \\ 0 & 1 \end{pmatrix}.$$

$$\Gamma = \kappa r^i \begin{pmatrix} 1 & 0 \\ 0 & \frac{N_c^2-2}{2(N_c^2-1)} \end{pmatrix} r^i$$

Total width → Im[V]

$$H_{\rm eff} = H_{\rm probe} - \frac{i}{2}\Gamma$$

Six collapse operators cover

- singlet → octet,
- octet → singlet
- octet → octet

$$\gamma \equiv \frac{g^2}{6\,N_c}\,{\rm Im}\int_{-\infty}^{+\infty} ds\,\langle T\,E^{a,i}(s,\mathbf{0})E^{a,i}(0,\mathbf{0})\rangle$$

$$\kappa \equiv \frac{g^2}{6\,N_c}\,{\rm Re}\int_{-\infty}^{+\infty} ds\,\langle T\,E^{a,i}(s,\mathbf{0})E^{a,i}(0,\mathbf{0})\rangle$$

OQS+pNRQCD Hamiltonian and collapse operators

N. Brambilla, M. A. Escobedo, J. Soto and A. Vairo, 1612.07248, 1711.04515

$$\boxed{\frac{d\rho_{\rm probe}}{dt} = -iH_{\rm eff}\rho_{\rm probe} + i\rho_{\rm probe}H^\dagger_{\rm eff} + \sum_n C_n\,\rho_{\rm probe}\,C_n^\dagger}$$

$$\boxed{\rho = \begin{pmatrix} \rho_s & 0 \\ 0 & \rho_o \end{pmatrix}}$$

$$C_i^0 = \sqrt{\frac{\kappa}{N_c^2-1}}\,r^i \begin{pmatrix} 0 & 1 \\ \sqrt{N_c^2-1} & 0 \end{pmatrix},$$

$$C_i^1 = \sqrt{\frac{(N_c^2-4)\kappa}{2(N_c^2-1)}}\,r^i \begin{pmatrix} 0 & 0 \\ 0 & 1 \end{pmatrix}.$$

Six collapse operators cover

- singlet → octet,
- octet → singlet
- octet → octet

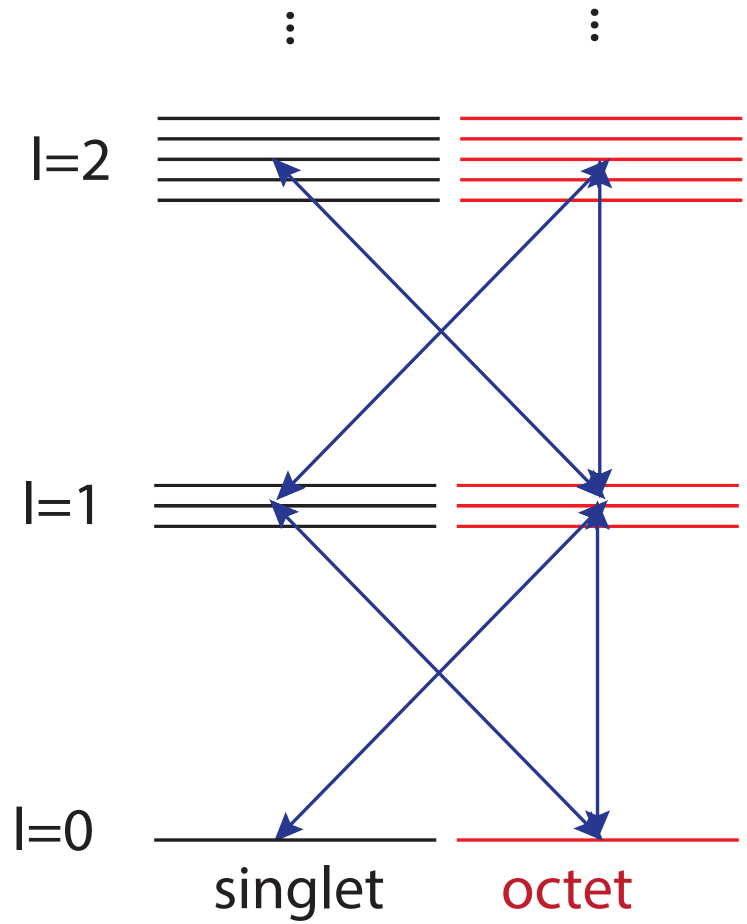

OQS+pNRQCD Hamiltonian and collapse operators

N. Brambilla, M. A. Escobedo, J. Soto and A. Vairo, 1612.07248, 1711.04515

$$\frac{d\rho_{\rm probe}}{dt} = -iH_{\rm eff}\rho_{\rm probe} + i\rho_{\rm probe}H_{\rm eff}^\dagger + \sum_n C_n\,\rho_{\rm probe}\,C_n^\dagger$$

$$\rho = \begin{pmatrix} \rho_s & 0 \\ 0 & \rho_o \end{pmatrix}$$

$$H_{\rm probe} = \begin{pmatrix} h_s & 0 \\ 0 & h_o \end{pmatrix} + \frac{r^2}{2}\gamma\begin{pmatrix} 1 & 0 \\ 0 & \frac{N_c^2-2}{2(N_c^2-1)} \end{pmatrix}$$

$$C_i^0 = \sqrt{\frac{\kappa}{N_c^2-1}}\, r^i \begin{pmatrix} 0 & 1 \\ \sqrt{N_c^2-1} & 0 \end{pmatrix},$$

$$\Gamma = \kappa r^i \begin{pmatrix} 1 & 0 \\ 0 & \frac{N_c^2-2}{2(N_c^2-1)} \end{pmatrix} r^i$$

$$C_i^1 = \sqrt{\frac{(N_c^2-4)\kappa}{2(N_c^2-1)}}\, r^i \begin{pmatrix} 0 & 0 \\ 0 & 1 \end{pmatrix}.$$

$$\gamma \equiv \frac{g^2}{6\,N_c}\,{\rm Im}\int_{-\infty}^{+\infty} ds\,\langle T\,E^{a,i}(s,\mathbf{0})E^{a,i}(0,\mathbf{0})\rangle$$

$$\kappa \equiv \frac{g^2}{6\,N_c}\,{\rm Re}\int_{-\infty}^{+\infty} ds\,\langle T\,E^{a,i}(s,\mathbf{0})E^{a,i}(0,\mathbf{0})\rangle$$

Six collapse operators cover

- singlet → octet,
- octet → singlet
- octet → octet

Values of $\hat{\kappa}$ and $\hat{\gamma}$ used

- We used NLO fits to recent lattice measurements of the heavy quark transport coefficient $\hat{\kappa} \equiv \kappa/T^3$. Note that this is related to the heavy quark diffusion constant D.
  - N. Brambilla, V. Leino, P. Petreczky, and A. Vairo, 2007.10078

N. Brambilla, V. Leino, P. Petreczky, and A. Vairo, 2007.10078

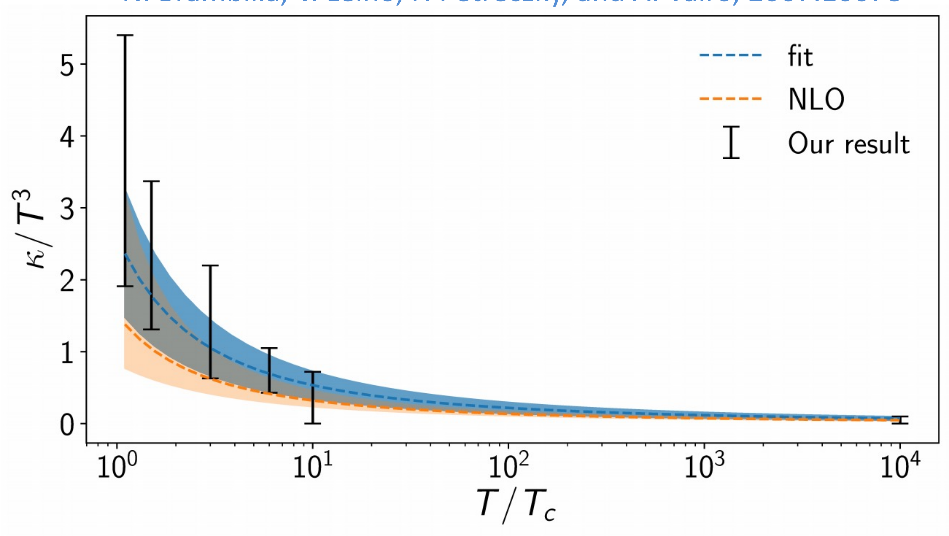

- The value of $\hat{\gamma} \equiv \gamma/T^3$ is less constrained, we vary it in the range -3.5 < $\hat{\gamma}$ < 0.
  - N. Brambilla, M. A. Escobedo, J. Soto and A. Vairo, 1612.07248.
  - N. Brambilla, M. A. Escobedo, J. Soto and A. Vairo, 1711.04515.
  - N. Brambilla, M. A. Escobedo, A. Vairo and P. Vander Griend, 1903.08063.

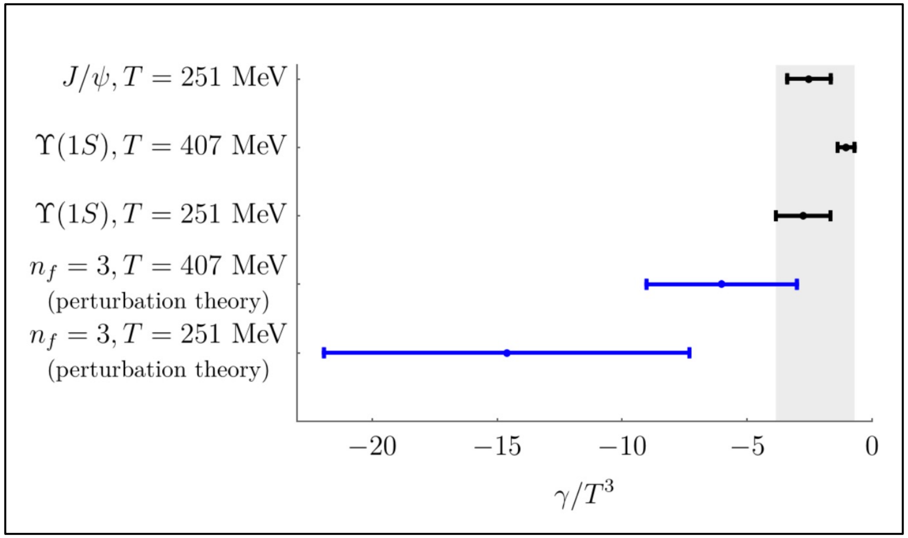

N. Brambilla, M. A. Escobedo, A. Vairo and P. Vander Griend, 1903.08063.

How can one numerically solve these equations?

$$\boxed{\frac{d\rho_{\rm probe}}{dt} = -iH_{\rm eff}\rho_{\rm probe} + i\rho_{\rm probe}H_{\rm eff}^\dagger + \sum_n C_n\,\rho_{\rm probe}\,C_n^\dagger}$$

- Each block of the density matrix in color space can be decomposed into orbital angular momentum blockwise.
- Upon truncating in angular momentum ($l \le l_{max}$) one can reduce both the singlet and octet blocks of the reduced density matrix to size $(l_{max}+1)^2$.
- One can then discretize the radial wavefunction (N = # of lattice points) and evolve the reduced density matrix using standard differential equation and matrix solvers gives $\sim N^2(l_{max}+1)^2$ matrix size.
- **Need to describe bound and unbound states with highly localized initial wave function, so the box must be large and have small lattice spacing → large N and large l_{max}.**
- As N and l_{max} become large, **the computation becomes very challenging**.
- **Need a better/faster method which we can easily parallelize.**

A parallelizable approach: Quantum trajectories

N. Brambilla, M.-A. Escobedo, M.S., A. Vairo, P. Vander Griend, and J.H. Weber, 2012.01240

$$\frac{d\rho_{\rm probe}}{dt} = -iH_{\rm eff}\rho_{\rm probe} + i\rho_{\rm probe}H^{\dagger}_{\rm eff} + \sum_n C_n\,\rho_{\rm probe}\,C^{\dagger}_n$$

Non-unitary "no jump" evolution

Can treat this "quantum jump" term stochastically

- Can be reduced to the solution of a large set of "quantum trajectories" in which we solve a 1D Schrödinger equation with a **non-Hermitian Hamiltonian $\boldsymbol{H_{\rm eff}}$**, subject to **stochastic quantum jumps**.
- The evolution with the non-Hermitian $H_{\rm eff}$ preserves the color and angular momentum state of the system (but not norm).
- Collapse/jump operators encode transitions between different color/angular momentum states (subject to selection rules).

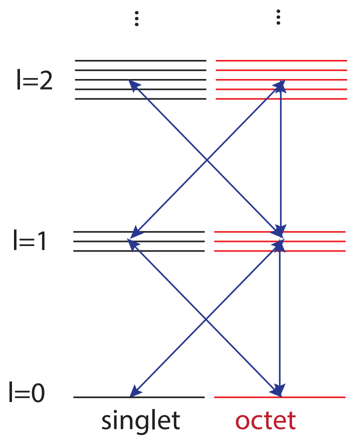

- For each **physical trajectory** (path through the QGP) we average over a large set of **<u>independent</u> quantum trajectories** → **Embarrassingly parallel**
- **Added benefit: Can describe all angular momentum states (no cutoff) .**

Initial bottomonium wavefunction

- We took the initial wavefunction to be given by a smeared delta function (local production due to large mass, Δ ~ 1/M) of the form

$$u_\ell(r, \tau = 0) \propto r^{\ell+1} \exp(-r^2/\Delta^2)$$

- For a given l, the **initial state is a quantum linear superposition** of the eigenstates of H.
- **Includes both bound and unbound states.**
- We took $\Delta = 0.2\, a_0$ which reproduces results obtained with a true delta to within 1%.

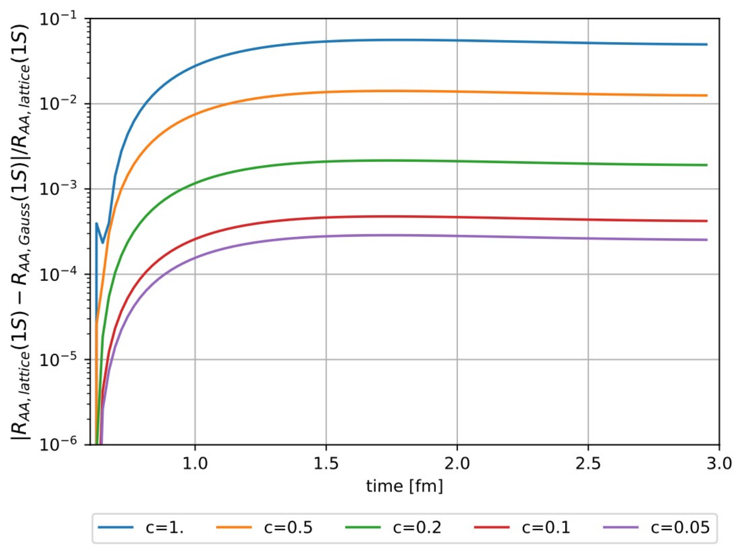

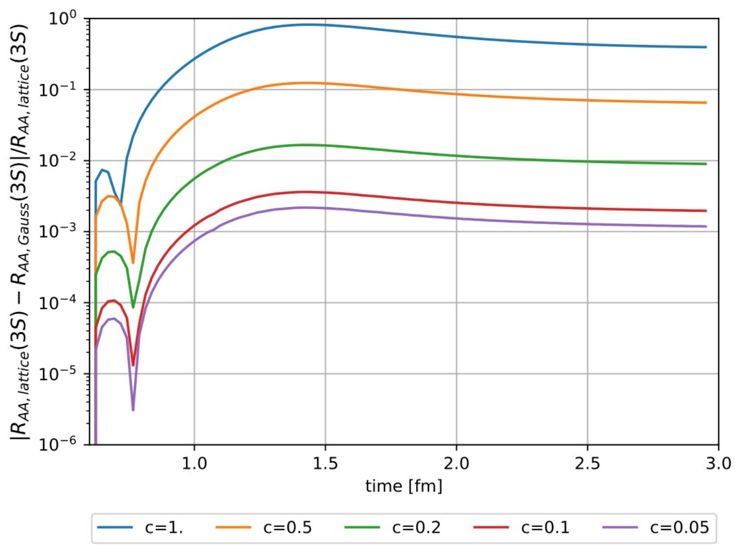

Computing survival probabilities with QTraj

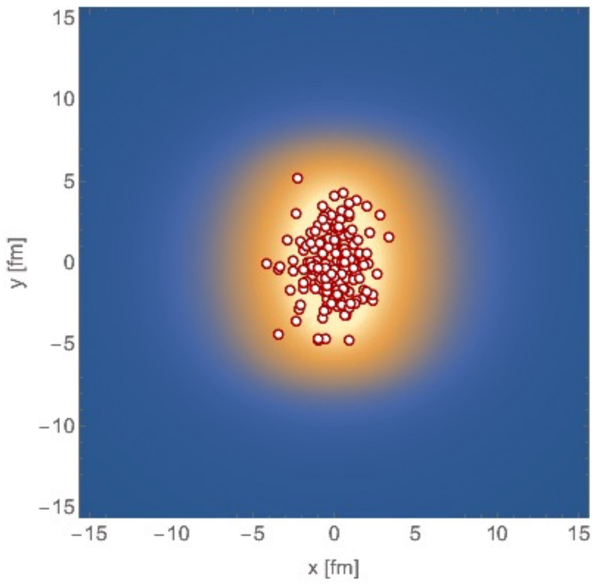

Survival probability

$$SP(n,l) = \frac{|\langle n,l|\psi(t_f)\rangle|^2}{|\langle n,l|\psi(t_0)\rangle|^2}$$

- Used $N = 4096$ points
- $L = 108\ a_0$
- $\Delta t = 2 \times 10^{-4}$ fm

- We sampled bottomonium production points and transverse momentum using **Monte-Carlo sampling**.
- Temperature evolution provided **by 3+1D anisotropic hydrodynamics** (good description of identified hadron spectra and anisotropic flow, see backup slides).
- We solved the **real-time 3D Schrödinger equation with a complex potential and stochastically sampled jumps** → Lindblad equation.
- We then solved for the **survival probability** of S- and P-wave states (see box to the left).

Feed-down implementation

$$\vec{N}_{\rm observed} = F\vec{N}_{\rm direct}$$

$$F = \begin{pmatrix} 1 & 0.2645 & 0.0194 & 0.352 & 0.18 & 0.0657 & 0.0038 & 0.1153 & 0.077 \\ 0 & 1 & 0 & 0 & 0 & 0.106 & 0.0138 & 0.181 & 0.089 \\ 0 & 0 & 1 & 0 & 0 & 0 & 0 & 0 & 0 \\ 0 & 0 & 0 & 1 & 0 & 0 & 0 & 0.0091 & 0 \\ 0 & 0 & 0 & 0 & 1 & 0 & 0 & 0 & 0.0051 \\ 0 & 0 & 0 & 0 & 0 & 1 & 0 & 0 & 0 \\ 0 & 0 & 0 & 0 & 0 & 0 & 1 & 0 & 0 \\ 0 & 0 & 0 & 0 & 0 & 0 & 0 & 1 & 0 \\ 0 & 0 & 0 & 0 & 0 & 0 & 0 & 0 & 1 \end{pmatrix}$$

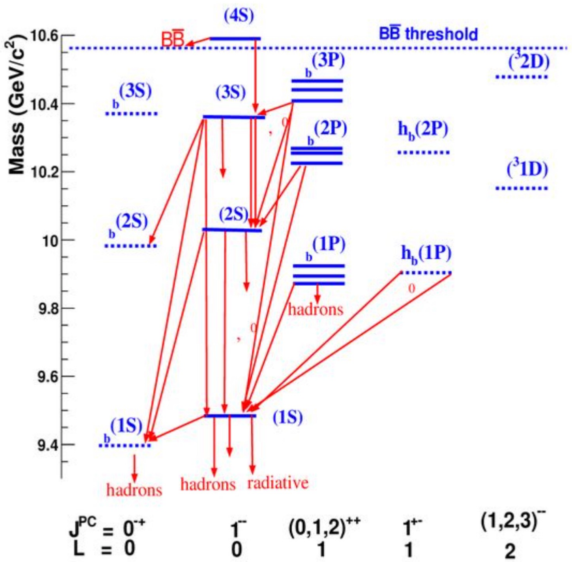

- $N_{\rm direct}$ corresponds to (N_{1S}, $N_{2S,}$ N_{1P} x 3, $N_{3S,}$ N_{2P} x 3, N_{2D})^T where, e.g., N_{1S} is the final number of Y(1S) states that can decay in the dilepton channel.

- $N_{\rm direct}$ can be obtained using <$N_{\rm bin}$(b)> * $\sigma_{\rm direct}$ * (Survival probability)

- After feed down, we then normalize to by the pp collision result scaled to AA → R_{AA}.

$$\boxed{R^i_{AA}(c) = \frac{(F\cdot S(c)\cdot\vec{\sigma}_{\rm direct})^i}{\sigma^i_{\rm exp}}}$$

OQS + pNRQCD predictions for R_{AA} vs N_{part}

N. Brambilla, M.-A. Escobedo, M.S., A. Vairo, P. Vander Griend, and J.H. Weber, forthcoming

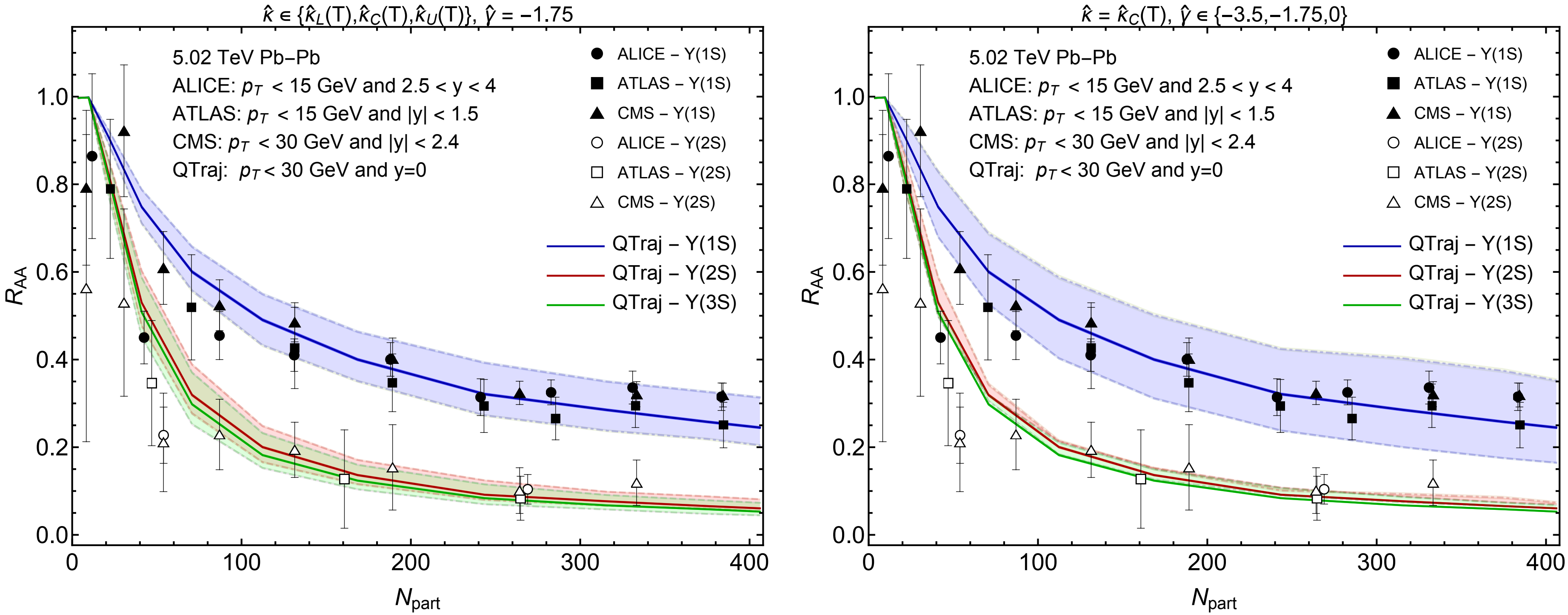

- **Left panel**: Result including feed down, when varying $\hat{\kappa}$ over the theoretical uncertainty.
- **Right panel**: Result including feed down, when varying $\hat{\gamma}$ over the theoretical uncertainty
- Statistical uncertainty associated with average over quantum trajectories is on the order of the line width.

OQS + pNRQCD predictions for R_{AA} vs N_{part}

N. Brambilla, M.-A. Escobedo, M.S., A. Vairo, P. Vander Griend, and J.H. Weber, forthcoming

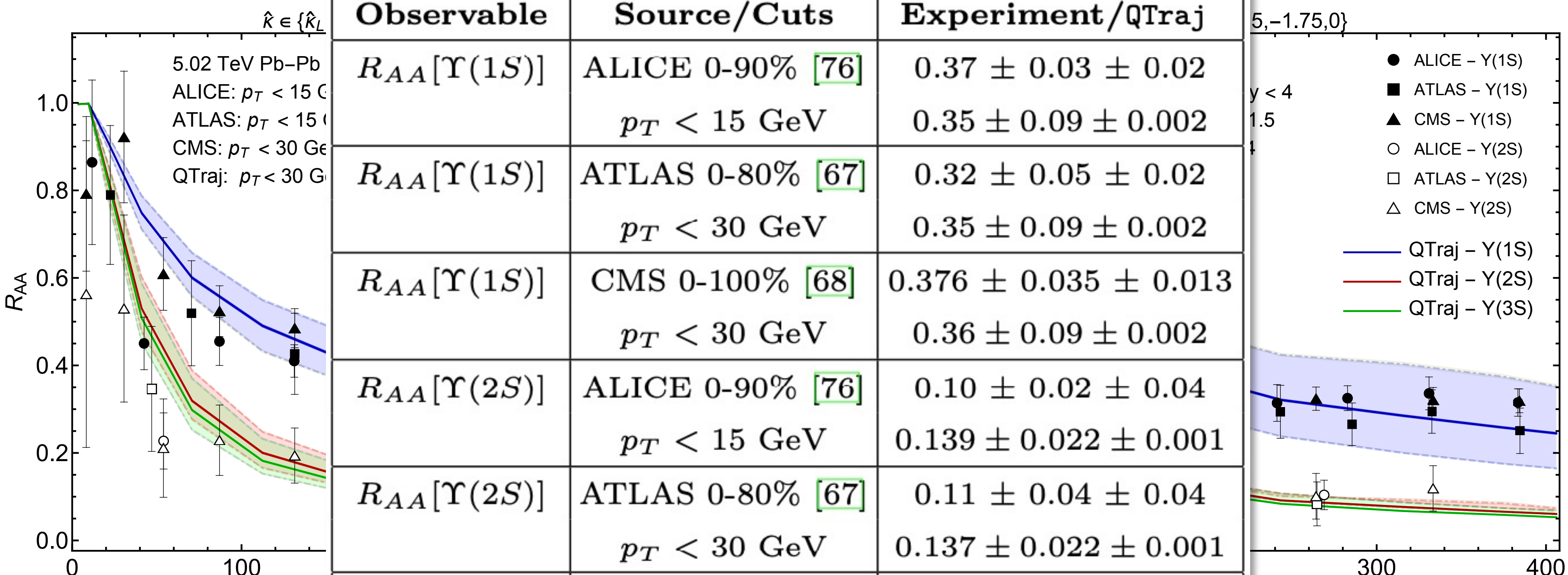

Observable	Source/Cuts	Experiment/QTraj
$R_{AA}[\Upsilon(1S)]$	ALICE 0-90% [76]	$0.37 \pm 0.03 \pm 0.02$
	$p_T < 15$ GeV	$0.35 \pm 0.09 \pm 0.002$
$R_{AA}[\Upsilon(1S)]$	ATLAS 0-80% [67]	$0.32 \pm 0.05 \pm 0.02$
	$p_T < 30$ GeV	$0.35 \pm 0.09 \pm 0.002$
$R_{AA}[\Upsilon(1S)]$	CMS 0-100% [68]	$0.376 \pm 0.035 \pm 0.013$
	$p_T < 30$ GeV	$0.36 \pm 0.09 \pm 0.002$
$R_{AA}[\Upsilon(2S)]$	ALICE 0-90% [76]	$0.10 \pm 0.02 \pm 0.04$
	$p_T < 15$ GeV	$0.139 \pm 0.022 \pm 0.001$
$R_{AA}[\Upsilon(2S)]$	ATLAS 0-80% [67]	$0.11 \pm 0.04 \pm 0.04$
	$p_T < 30$ GeV	$0.137 \pm 0.022 \pm 0.001$
$R_{AA}[\Upsilon(2S)]$	CMS 0-100% [68]	$0.117 \pm 0.019 \pm 0.022$
	$p_T < 30$ GeV	$0.148 \pm 0.022 \pm 0.001$
$R_{AA}[\Upsilon(3S)]$	CMS 0-100% [68]	$0.022 \pm 0.016 \pm 0.038$
	$p_T < 30$ GeV	$0.138 \pm 0.008 \pm 0.001$

- **Left panel**: Resu ... l uncertainty.
- **Right panel**: Res ... al uncertainty
- Statistical uncertainty associated with average over quantum trajectories is on the order of the line width.

2S/1S and 3S/1S double ratios

N. Brambilla, M.-A. Escobedo, M.S., A. Vairo, P. Vander Griend, and J.H. Weber, forthcoming

2S/1S

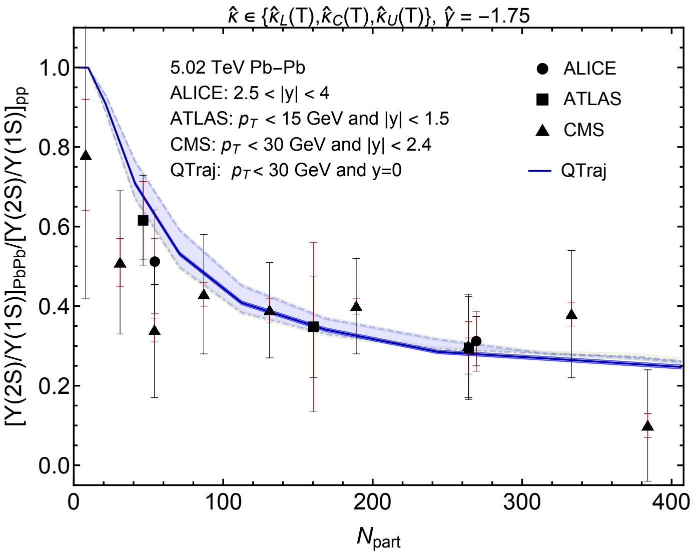

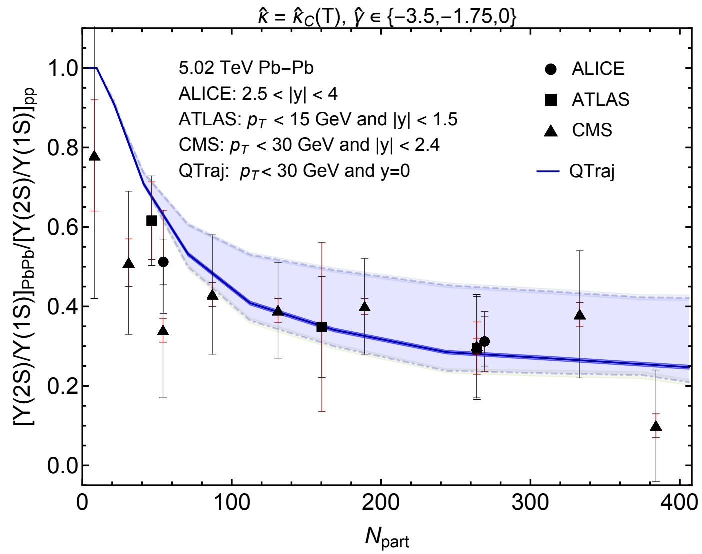

3S/1S

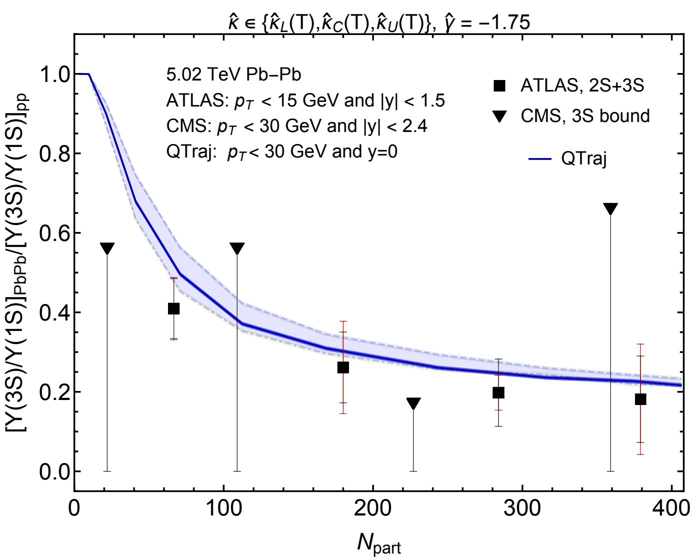

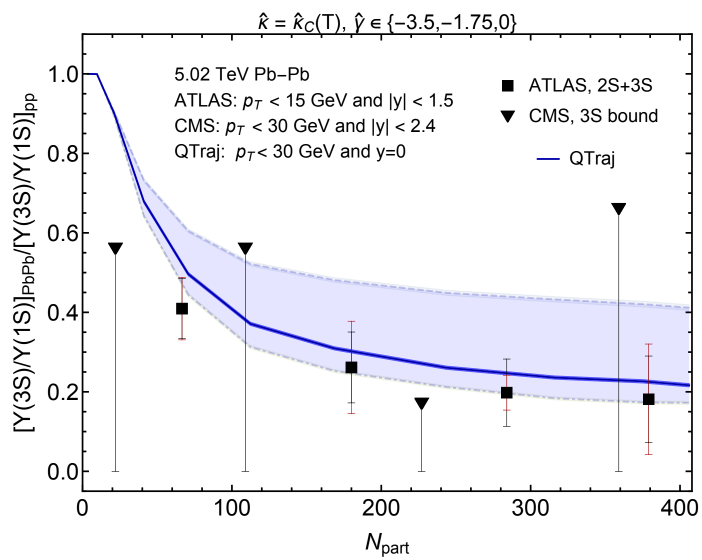

R_{AA} vs transverse momentum

N. Brambilla, M.-A. Escobedo, M.S., A. Vairo, P. Vander Griend, and J.H. Weber, forthcoming

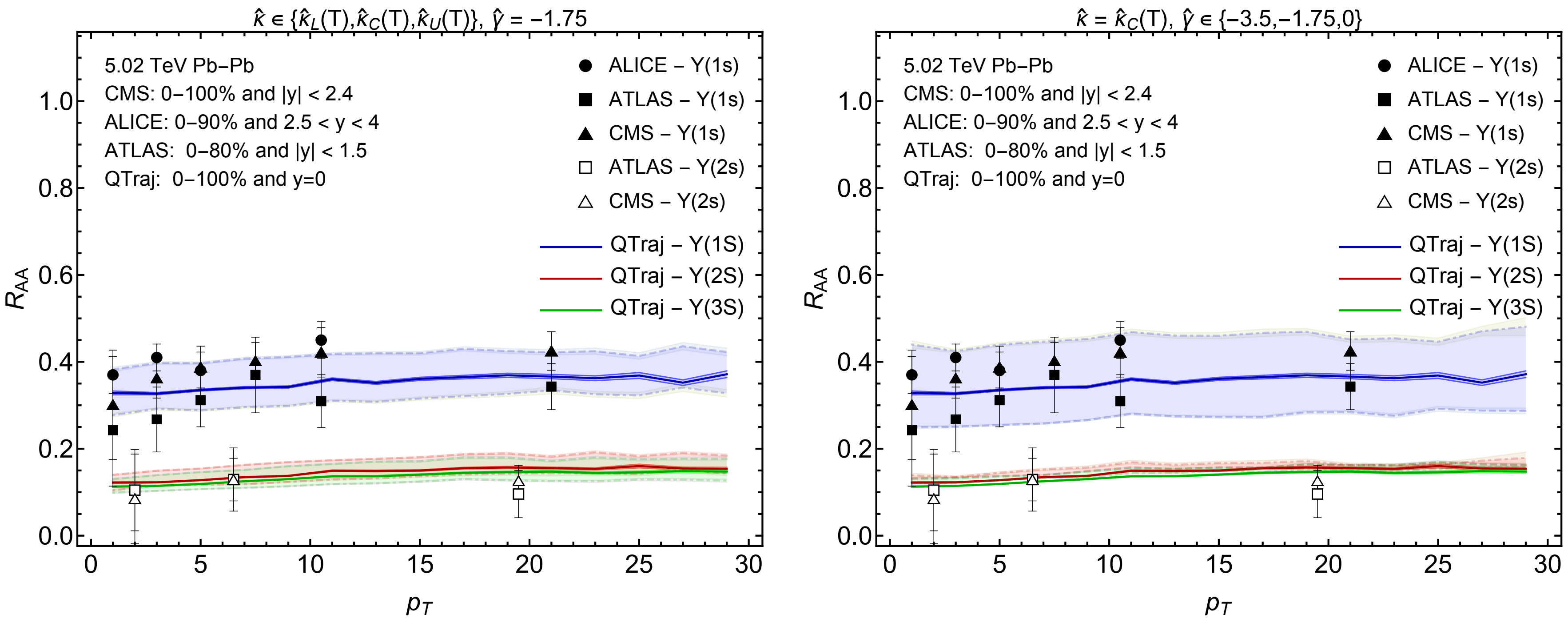

- QTraj predictions consistent with experimental observations.
- Very flat. Small decrease comes from longer time spent in the QGP.
- Once again, larger variation from variation of $\hat{\gamma}$.

2S/1S ratio vs transverse momentum

N. Brambilla, M.-A. Escobedo, M.S., A. Vairo, P. Vander Griend, and J.H. Weber, forthcoming

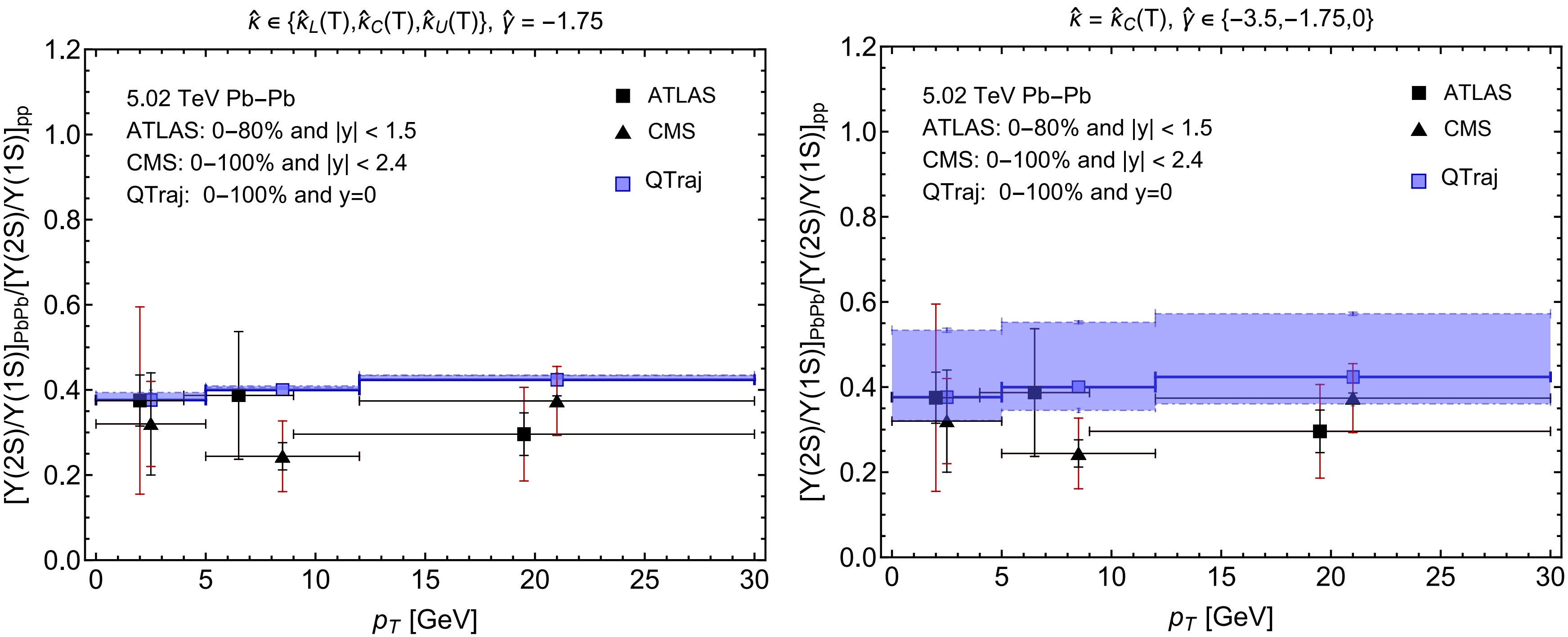

- Result does not depend on choice of κ, however, we see larger variation when varying γ; **value of $\gamma = -3.5$ has tension with data**

- **This offers some hope to constrain this transport coefficient from 2S/1S double ratio data.**

Momentum-space anisotropies

4d flow tomography

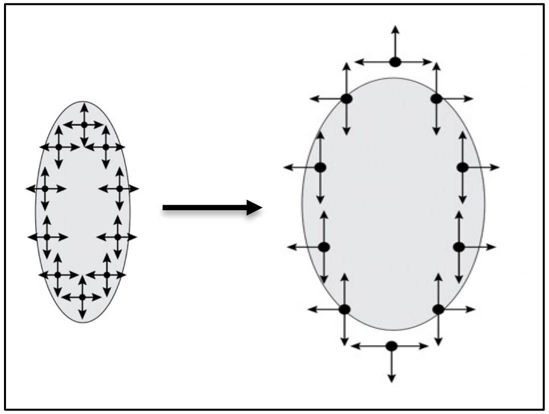

- Bottomonium probably doesn't flow in the "collective flow" sense.
- However, there can be momentum-space anisotropies induced by path-length differences in suppression along the short and long sides of the QGP.

Cern Courier, Fall 2019

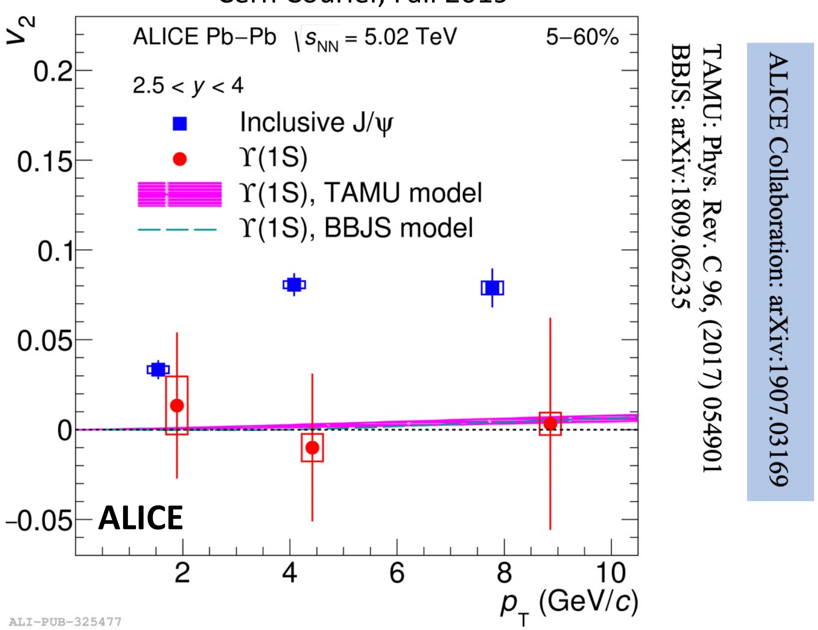

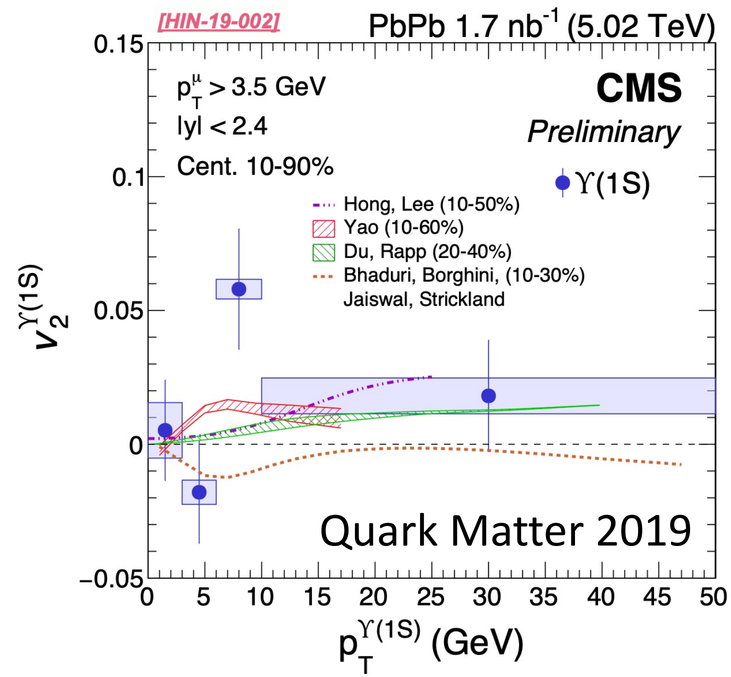

Momentum-space anisotropies

N. Brambilla, M.-A. Escobedo, M.S., A. Vairo, P. Vander Griend, and J.H. Weber, forthcoming

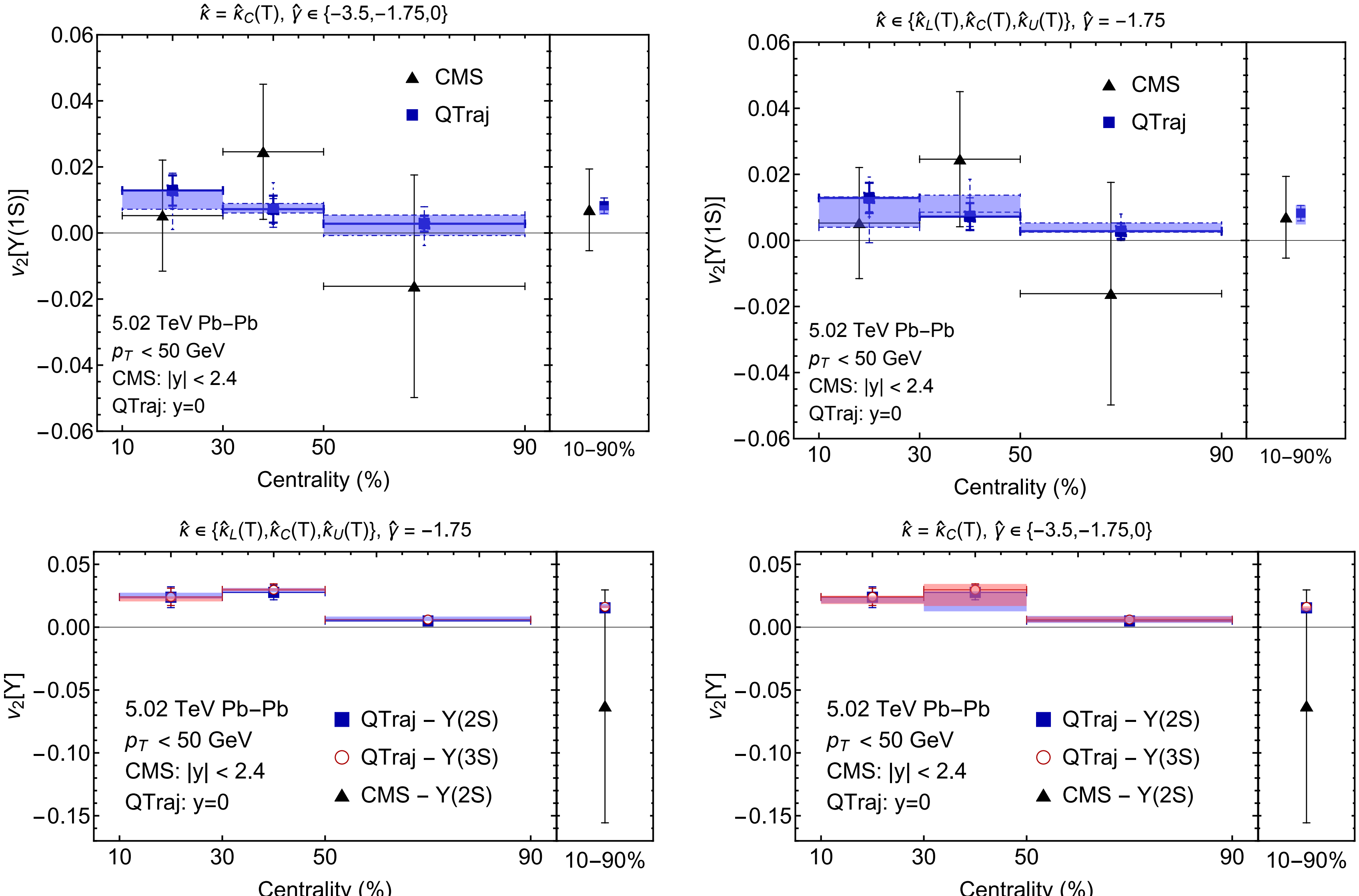

Momentum-space anisotropies

N. Brambilla, M.-A. Escobedo, M.S., A. Vairo, P. Vander Griend, and J.H. Weber, forthcoming

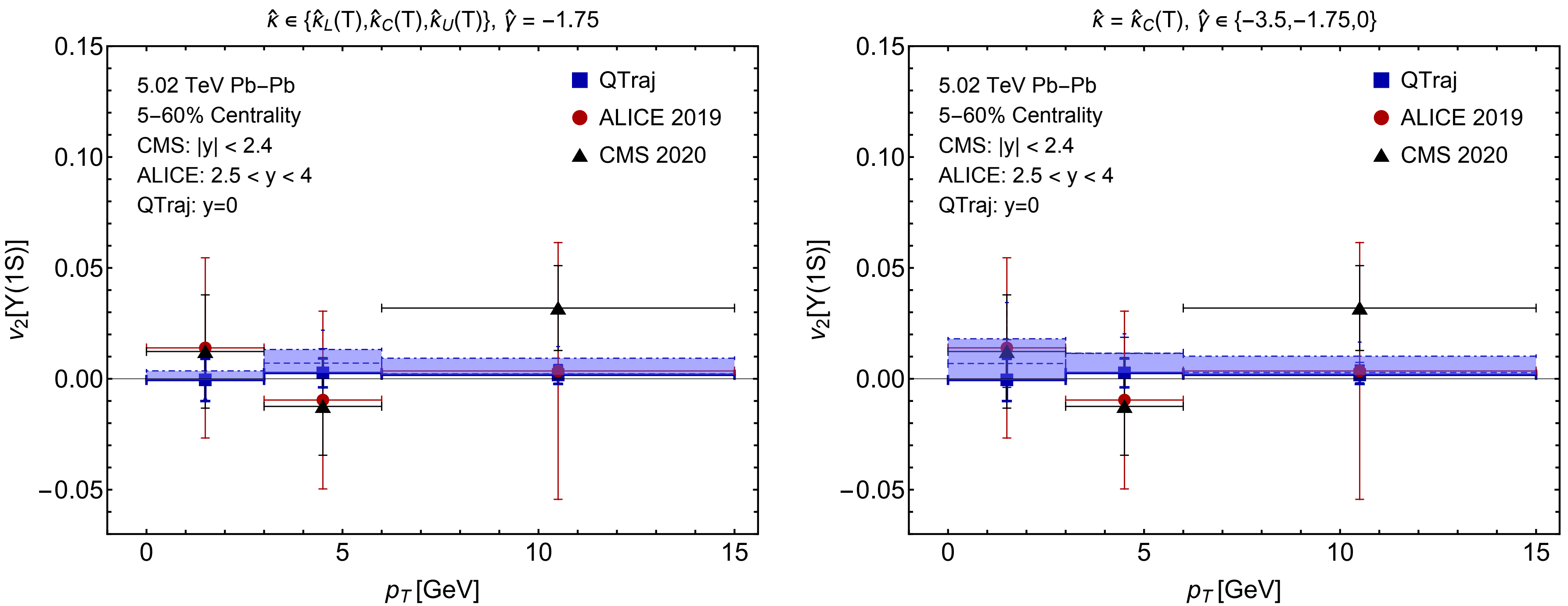

- Υ(1S) v_2 due to path length differences in suppression is small.
- **Qtraj predicts $|v_2[\Upsilon(1s)]|$ <~ 0.02 at all p_T.**
- Magnitude is consistent with prior works.
- Data have large uncertainties, hopefully more statistics in the future.

Conclusions and Outlook

- OQS + pNRQCD works very well to describe the suppression vs N_{part} and p_T, double ratios, and "flow" seen at LHC.
- **First full 3D quantum and non-abelian treatment within OQS.**
- Transport coefficients used were **constrained by independent lattice measurements.**
- Demonstrated that Upsilon R_{AA} and double ratios can be used to provide **experimental constraints on these transport coefficients**.
- The **quantum trajectory algorithm** (implemented in QTraj) allowed us to **include effect of quantum jumps** between color and angular momentum states in a **computationally scalable manner**.
- Code will be publicly released (GPLv3 license) along with with documentation (Computer Physics Communications) in the next weeks.
- One outstanding issue is the transition to low-temperature bottomonium dynamics ($T < 200 - 250\ \mathrm{MeV}$). Different ordering of scales, $T \lesssim E$ → **work in progress**.

Additional slides

Dependence on T_f

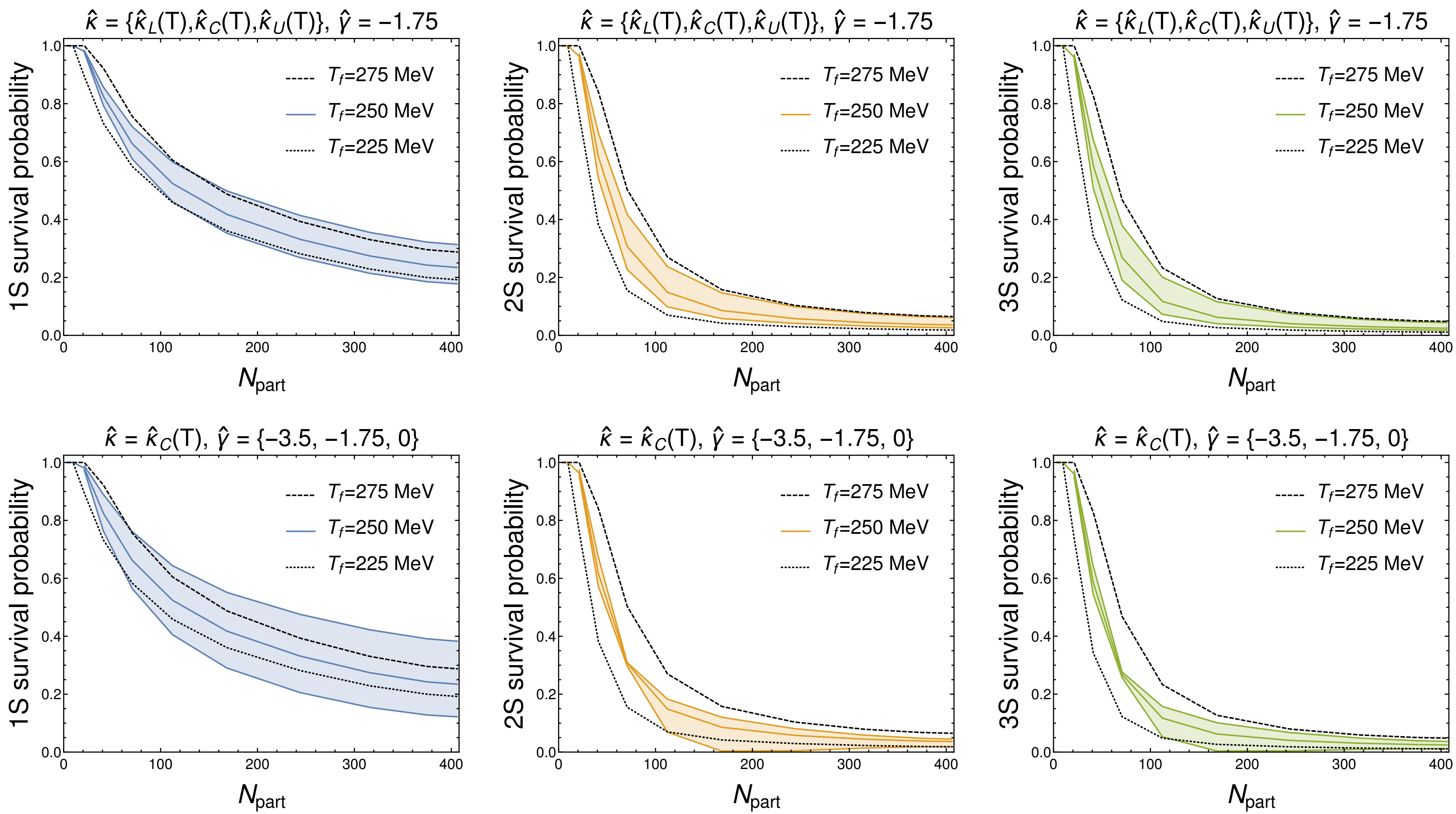

3+1D hydrodynamical background

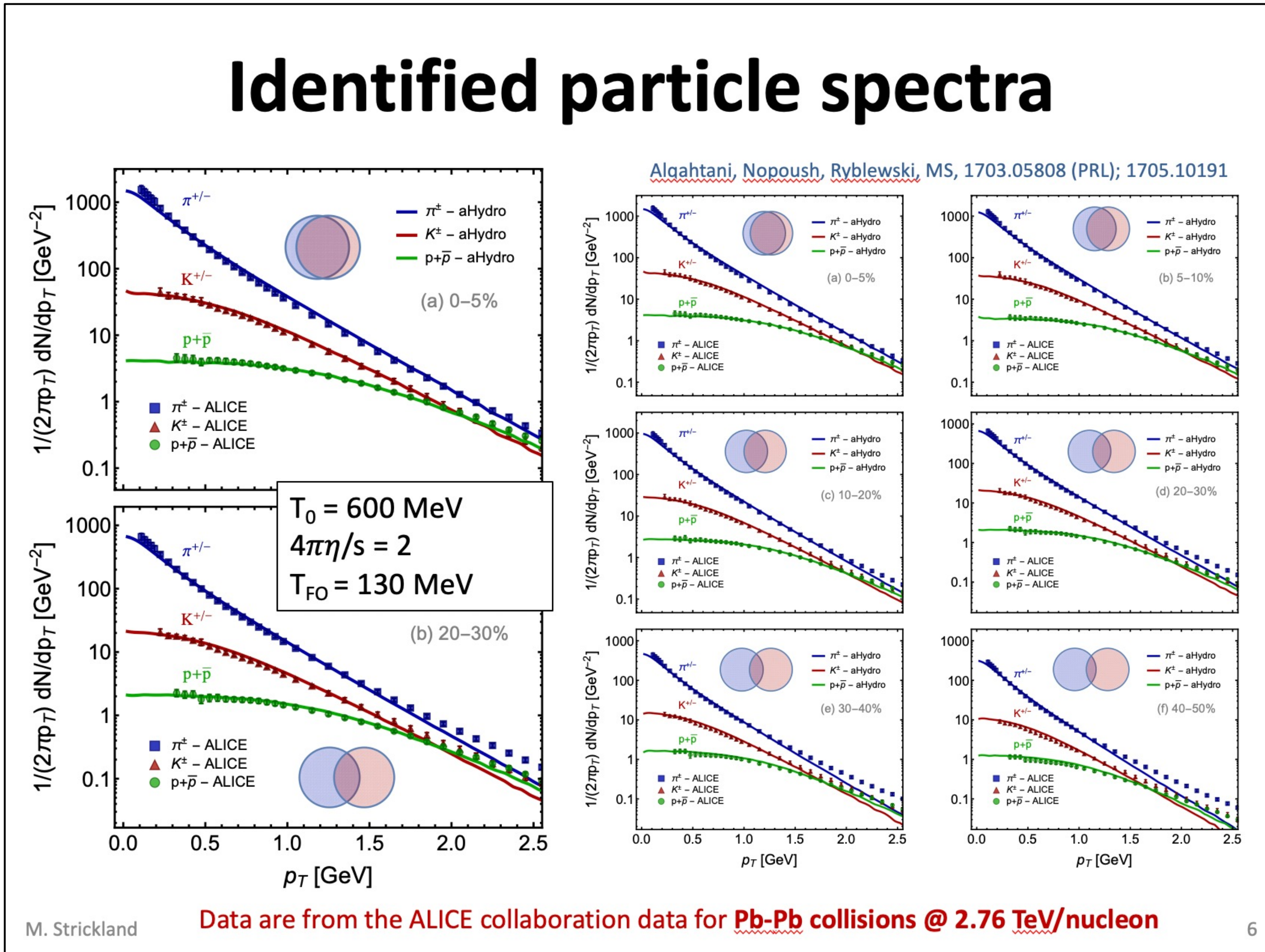

- We use a 3+1D dissipative code for the hydro background (quasiparticle anisotropic hydrodynamics)
- Has been tuned to RHIC and LHC heavy ion collisions
- Reproduces spectra, multiplicities, identified elliptic flow of light hadrons, HBT radii, etc.

For 5.02 TeV, T_0 = 630 MeV @ t_0 = 0.25 fm/c